

Ground-measured spectral signatures as indicators of ground cover and leaf area index: the case of paddy rice

K. Vaesen*, S. Gilliams, K. Nackaerts, P. Coppin

Laboratory for Forest, Nature and Landscape Research, Vital Decosterstraat 102, B-3000 Leuven, Belgium

Received 22 September 1999; received in revised form 24 July 2000; accepted 25 September 2000

Abstract

A methodology is described to use spectral signatures as indicators of the vegetative status in rice paddy cultures. Ground cover and leaf area index (LAI), considered as indicators of above-ground biomass, and were measured in the field using indirect techniques of digitized close-range vertical photography and Licor 2000 instrument readings, as well as direct destructive sampling. Simultaneously, field reflectance values were collected over specific spectral bandwidths using a hand-held radiometer. Several vegetation indices were derived from these spectral measurements and their predictive power (individually or in combination) with respect to field-measured ground cover and LAI quantified. The additional effects of plant chlorophyll content, paddy depth, water sediment load, and bottom layer color were also investigated. None of these variables added significantly to the predictive power of the models. The models were refined for intra-seasonal variability and a new growth-stage-dependent variable improved the models' predictive capabilities.

The results demonstrated that the monitoring of paddy rice crop status by means of its spectral signatures appears very promising. © 2001 Elsevier Science B.V. All rights reserved.

Keywords: Paddy rice; Leaf area index; Vegetation indices; Floodwater reflectance; Irrigation

1. Introduction

According to the FAO, rice is the most important world food crop. In 1993, rice was the principal food consumed by about 2.9 billion people living in 33 countries and was one of the five major foods consumed by a further 700 million people living in another 35 countries (FAOSTAT, 1998). Resolving

the specific problems in monitoring paddy rice remains a crucial factor in outlining an efficient water management policy in dry areas. Instantaneous estimates of biomass production can play an important role in arranging water distribution and irrigation requirements.

Good indicators of biomass production are ground cover (proportion of ground area covered by leaves) and leaf area index (LAI, the one-sided proportion of leaf area per unit ground area). Good estimates of actual biomass, ground cover and LAI have been derived from spectral measurements (Bouman et al., 1992; Leblon et al., 1991; Clevers, 1989). Predictive models of crop status (production and phenology) based on remotely sensed information, are potentially

* Corresponding author. Present address: Department of Land Management, Faculty of Agricultural and Applied Biological Sciences, Katholieke Universiteit Leuven, Vital Decosterstraat 102, 3000 Leuven, Belgium. Tel.: +32-16-32-97-49; fax: +32-16-92-97-60.
E-mail address: krist.vaesen@agr.kuleuven.ac.be (K. Vaesen).

useful because:

They allow fast, non-destructive and relatively cheap characterization of crop status (Bouman, 1995).

Model outputs (LAI, ground cover, ...) can be used in growth simulation models (ten Berge et al., 1995).

Spatial extrapolation to regional level using satellite imagery becomes feasible, for example rice (Ishiguro et al., 1993).

Model results are objective and repeatable.

The study of various biophysical plant features by remotely sensed data is complex, because the reflectance of a vegetative canopy is determined not only by plant morphology and phenology but also by soil characteristics (Huete and Jackson, 1985), irradiation, observation angle, and atmospheric condition. In order to maximize the contribution of vegetation reflectance information and to minimize the effects of exogenous factors, several vegetation indices (VIs) were developed during the last decades (Wallace and Campbell, 1989). Vegetation indices are based on the premise that the spectral behavior of vegetation is correlated with distinct biophysical processes and characteristics. Red light, for example, is strongly absorbed by chlorophyll, resulting in small reflectance values. Very-near-infrared (VNIR) energy, on the other hand is strongly reflected due to micro-cellular structures in leaf material. The focusing of the multispectral signal by combination of responses in different spectral regions, in the format of a ratio, or as a linear transformation, may therefore yield a more accurate estimate of biophysical plant parameters while reducing the impact of exogenous factors.

Though this research deals primarily with remotely sensed data obtained by a hand-held radiometer, for which atmospheric and viewing geometry effects are negligible, VIs remain valuable because they compensate for or stabilize variations in soil characteristics and irradiance.

One of the first operationally implemented VIs was the Rouse vegetation index, RVI (Rouse et al., 1973):

$$\text{RVI} = \frac{\rho_{\text{ir}}}{\rho_{\text{r}}} \quad (1)$$

where ρ_{r} is the red reflectance and ρ_{ir} the VNIR reflectance.

RVI was later modified to the normalized difference vegetation index or NDVI by the same authors (Rouse et al., 1973):

$$\text{NDVI} = \frac{\rho_{\text{ir}} - \rho_{\text{r}}}{\rho_{\text{ir}} + \rho_{\text{r}}} \quad (2)$$

Both RVI and NDVI are based on the marked contrast between low reflectance of healthy green vegetation in the visible red and high reflectance in the VNIR regions, which is nearly absent in the spectral behavior of soils.

To correct further for soil interferences, Wiegand and Richardson (1987) introduced the perpendicular vegetation index or PVI, also, requiring bare soil data:

$$\text{PVI} = \sqrt{(\rho_{\text{ir}} - \rho_{\text{ir,s}})^2 + (\rho_{\text{r}} - \rho_{\text{r,s}})^2} \quad (3)$$

where $\rho_{\text{r,s}}$ is the red reflectance of a bare soil and $\rho_{\text{ir,s}}$ the VNIR reflectance of a bare soil. PVI calculates the deviation of the reflective signal of vigorous vegetation that is less sensitive to the underlying soil type.

The weighted difference vegetation index or WdVI (Clevers, 1989) normalizes specifically for soil moisture influences:

$$\text{WdVI} = \rho_{\text{ir}} - \left(\frac{\rho_{\text{ir,s}}}{\rho_{\text{r,s}}} \right)^2 \rho_{\text{r}} \quad (4)$$

Various models have been developed to correlate these VIs with relevant crop biophysical characteristics such as ground cover and LAI. Kumar and Montheith (1981), Steven et al. (1985) and Gallo et al. (1985) demonstrated a strong correlation between the intercepted fraction of photosynthetically active radiation (Fpar) and RVI or NDVI. Casanova et al. (1998) proposed the following model to link Fpar to LAI:

$$\text{Fpar} = 1 - e^{-K \times \text{LAI}} \quad (5)$$

where K is the extinction coefficient.

A serious limitation of this model is the need to determine K empirically for the various growth stages.

The Clevers leaf area index by reflectance (CLAIR) model (Clevers et al., 1991) establishes a direct relationship between WdVI and LAI according to the following formula:

$$\text{LAI} = \frac{-1}{\alpha} \left(1 - \frac{\text{WdVI}}{\text{WdVI}_{\infty}} \right) \quad (6)$$

where α is the constant and $WDVI_{\infty}$ the asymptotic (with respect to LAI) threshold value for $WDVI$. A similar limitation exists as with the previous model: both α and $WDVI_{\infty}$ must be determined empirically.

Paddy rice differs from other crops in that the floodwater may affect the spectral reflectance. This prohibits the unconditional use of VIs for monitoring rice biomass production (Patel et al., 1985; Gilabert and Meliá, 1990a,b). As primary objective, the present study will study the relationships between paddy rice spectral information and its ground cover and LAI. Additional objectives were to quantitatively define the impact of biophysical parameters such as water depth, water clarity, water background color, plant chlorophyll content, rice cultivar, nitrogen treatment, on these relationships. The results refer to models that depict the relationship between spectral data collected with a hand-held radiometer and above-ground biomass of paddy rice crops, but where positive, the link to satellite-based spectral data will be investigated.

2. Methods and material

2.1. Research site

This study was carried out at the Ndiaye region in Northern Senegal ($16^{\circ}13'N$ – $16^{\circ}15'W$) on fields of WARDA, the West African Rice Development Association. The climate is semi-arid with a long dry season (mid-November–mid-July), a short rainy season (mid-July–mid-November) characterized by a low and irregular rainfall, and an average growing period of less than 75 days. The region holds a major potential for irrigated rice, due to abundant water resources from the Senegal river and the clayey character of the alluvial. Consequently, over 78% of the agricultural land in the Senegal River Delta is occupied by paddy rice *Oryza sativa* L., with average yields of 4–4.5 t/ha.

2.2. Experimental design

The experimental design comprised 22 square ($10\text{ m} \times 10\text{ m}$) paddy plots of uniform soil texture

(Fig. 1), selected to meet the following objectives:

1. The range of dependent variables, LAI and ground cover, is broad enough to allow development and testing of robust relationships.
2. Values for $\rho_{r,s}$ and $\rho_{ir,s}$ (Eq. (3)) and their ratio (Eq. (4)) can be derived.
3. The dependence of the models on rice cultivar can be tested.
4. The influence of water turbidity and water depth can be determined.
5. The impact of bottom layer color and leaf chlorophyll content can be verified.
6. Models solely based on spectral information can be tested for their predictive power against models comprising mixed (spectral and biophysical) data.

Sixteen plots were used in a first modeling exercise (objectives 1, 3, 4 and 6), two in a second (objective 2), and four in a third (objective 5).

Rice seedlings, which had been initially grown in pots for 21 days, were transplanted to all experimental plots on 11 August 1997. In the first exercise, eight plots were planted with rice cultivar Sahel 108 and eight with cultivar Jaya, at an inter-row distance of 20 cm. To broaden the variability of the measured variables, four different N treatments were applied: 0, 60, 120 and 180 kg/ha. The fertilizer was applied at specified phenological stages of rice in fractions of 60 kg/ha each. Thus for 60 kg N/ha, a single dose was applied once the rice was growing vigorously after transplanting (vegetative status). For the 120 kg N/ha input, an additional 60 kg dose was applied around primary panicle development (reproductive stage). For the 180 kg N/ha input, a third 60 kg/ha dose was given at the beginning of the maturation stage. Thus for each cultivar there were two plots with the same N input. The separating factor between the two replicates at the time of data collection, however, was the water turbidity level. In one of the two plots, sediments (soil) were stirred prior to measurement. In the other, the plot was left undisturbed.

The second trial was set up to create a “water line” analogous to the soil line concept (Clevers, 1989). One of two non-cropped plots (water layers) had its water layer disturbed by agitation at the time of data collection, resulting in a suspended sediment load. The other remained clear. Red and VNIR reflectances were measured weekly and a regression line was fitted in

Trial 1

V1-N1 turbid	V1-N2 turbid	V1-N1 clear	V1-N2 clear
V1-N3 turbid	V1-N4 turbid	V1-N3 clear	V1-N4 clear
V2-N1 turbid	V2-N2 turbid	V2-N1 clear	V2-N2 clear
V2-N3 turbid	V2-N4 turbid	V2-N3 clear	V2-N4 clear

TRIAL 2

NC turbid
NC clear

TRIAL 3

NC white	CV1 white
NC black	CV1 black

V1= Cultivar 1 (Sahel108)

V2= Cultivar 2 (Jaya)

N1 = nitrogen supply of 0kg/ha over growing season

N2 = nitrogen supply of 60kg/ha over growing season

N3 = nitrogen supply of 120kg/ha over growing season

N4 = nitrogen supply of 180kg/ha over growing season

NC = non-cropped

C = cropped

White = bottom covered with white plastic sheet under floodwater layer

Black = bottom covered with black plastic sheet under floodwater layer

Fig. 1. Experimental design.

two-dimensional space. The depth of the water layer was varied between 5 and 25 cm, as the work of Casanova et al. (1998) pointed to the influence of water depth on VNIR reflectance.

The third modeling exercise addressed the effect of background soil color on spectral measurements in flooded crops. Two plots had their soil covered with white, two others with black plastic sheets. Of each, one was planted with rice (Sahel 108, 60 kg N), the other was not.

2.3. Data collection

The measured parameters could be grouped into three categories. First, those used to establish basic relationships between spectral information and biophysical status (a–c). Second, those intended to con-

tribute to a refinement of the basic relationships (d and e). Third, those used to verify the statistical significance of the effect of paddy rice background color on these relationships (f). All parameters, except for (f), were measured weekly between 18 August (transplanting date) and 20 November 1997 (harvest date). They encompassed.

2.3.1. Reflectance

Measurements were taken with a hand-held multi-spectral Cropscan radiometer (Cropscan Inc, 1993). Although the instrument collected information in eight separate spectral channels, we used only channel 5 (centered at 0.66 μm) and channel 8 (centered at 0.81 μm) as red and VNIR inputs to the computation of the various VIs (Eqs. (1)–(4)). Single readings were always taken horizontally to the canopy and at

2 m above the ground between 9:00 and 10:00 h, the latter to avoid hotspot effects occurring mostly from 11:00 and 15:00 h. They were done at six fixed sample points towards the middle of the plot in order to minimize variability and edge effects. There were no wind effects on leaf angle, leading to different spectral responses, during the period of measurement.

2.3.2. Leaf area index

As described in the manual (Licor, 1992), LAI cannot be measured with the Licor LAI-2000 when soil cover is small just after transplanting. The LAI-3000 (Licor, 1990) was therefore used to directly measure leaf area, following destructive sampling and this in very young, open rice canopies (LAI below a critical value of 1). Five plants per plot, representing a ground area of 0.2 m² were randomly selected. All leaves were removed from the plants and immediately scanned by the LAI-3000.

For more developed canopies (LAI > 1), an indirect method was applied using the LAI-2000 (Licor, 1992). This instrument contains five concentric optical detectors, which measure the spherical distribution of light. The ratio of above to below light intensity measurements, corresponds to the probability of non-interceptance of light by the canopy. Based on a Poisson light distribution model, and the assumptions of randomly distributed, randomly oriented and absolute absorbing foliage, this probability is converted to LAI.

2.3.3. Ground cover

An estimate of ground cover (ratio of area covered by vegetative biomass over total area) was derived from 35 mm photography using a 38–60 mm zoom lens. The camera was mounted, downward facing, on a horizontal arm at a height of 2 m above the sampling point so that its coverage was about 1 m². The negatives were digitized using a 35 mm slide scanner at 560 dots per inch for a resolution of approximately 2 mm. This resolution allowed identification of features with minimum dimensions up to 5 mm. This allowed identification of features with minimum dimensions up to 5 mm, considered acceptable for this study. IDRISI software (Idrisi, 1997) was used to classify the digital photographs in the binary classes “vegetation present” and “vegetation absent” using a maximum likelihood classification routine. The ratio

of “vegetation present” pixels to total number of pixels provided the estimate of ground cover.

2.3.4. Chlorophyll content

Sunlight is mainly absorbed by chlorophyll, so, inclusion of chlorophyll content to any model relating spectral information to biophysical data might strengthen its descriptive and predictive potential. The SPAD-502 instrument (Soil-Plant Analysis Development Section, Minolta, Osaka, Japan) was used to determine chlorophyll content of rice leaves. An average value per plot was derived from five plants per plot and three leaves per individual plant.

2.3.5. Paddy characteristics

Because of the characteristic properties of water in terms of absorption, transmittance and reflectance of solar energy, depth and turbidity (sediment load) were assessed in every data collection cycle. A ruler was used to measure water depth at the same six points per plot used for the Cropscan data collection. Water clarity was categorized as either undisturbed or disturbed.

2.3.6. Background color

Because the significance of background color (related to soil type) in paddy rice plot models was unclear, a third independent trial was added to the experimental design (Fig. 1). The values of this variable were bright and dark, obtained by attaching respectively a white and black plastic to the paddy soil, so that they laid at the bottom of the water layer.

2.4. Data analysis

In the first phase, analysis consisted of establishing relationships, via least squares linear regression procedures, between measures of LAI and/or ground cover (dependent variables) and spectral measurements of VIs (independent variables). Significance tests for categorical variables (rice cultivar, water turbidity, paddy background color, N treatment) were included to evaluate if additional data sets were warranted. In the second phase, the explanatory power of additional parameters was investigated by a stepwise regression. A first group of such additional parameters comprised the biophysical properties leaf chlorophyll content and paddy depth. A second set consisted of the

individual spectral channels of the Cropscan instrument which were used to compute the VIs.

These variables were introduced together with the VIs as independent variables in a forward stepwise regression, with the $C(p)$ coefficient (Neter et al., 1996; Salvador and Pons, 1998) as criterion for ranking the independent variables and the F -statistics as descriptor of the sequential variation-explicative power of the independent variables. Two-way interactions for simple correlation were included as well in the analysis. This stepwise procedure allowed formulating models that explained the maximum overall variability but not necessarily comprised the predictor variables with the highest F -scores. The stepwise procedure also corrected for multicollinearity between variables through their removal from the model.

Casanova et al. (1998) found that a two-step model linking spectral information in the form of VIs (via F_{par}) to LAI was only possible by introducing a growth-stage coefficient (extinction coefficient K in Eq. (6)). This suggested the need for an analogous variable derived from the available data set. Such a variable must capture the spectral shifts associated with the development of the rice crop, especially since Gilabert and Meliá (1990b) have shown a large intra-seasonal temporal variability of the spectral response of flooded rice using Landsat Thematic Mapper

data. We therefore derived similar temporal spectral profiles from our Cropscan spectral database, and grouped these according to development stage as observed in the N fertilization trial. Each stage was assigned a group number characterizing the growth-stage-dependent variable. Ultimately, the variable was included in the stepwise regression for model improvement.

3. Results and discussion

3.1. VIs and ground cover

Fig. 2 presents the time course of ground cover for Sahel 108 with turbid floodwater over the entire growing season for four N fertilization levels. It did not correspond with the expected ascending trend, with saturation at maturity, in any of the experimental plots.

Regression analysis between ground cover and the vegetation indices RVI, NDVI, PVI and WDI confirmed the trends found by Casanova et al. (1998), though less explicitly: Casanova reported adjusted R^2 's to be larger than 0.67 for all cases, while values found in this study ranged between 0.27 and 0.68 only. To allow direct comparison, models identical to those

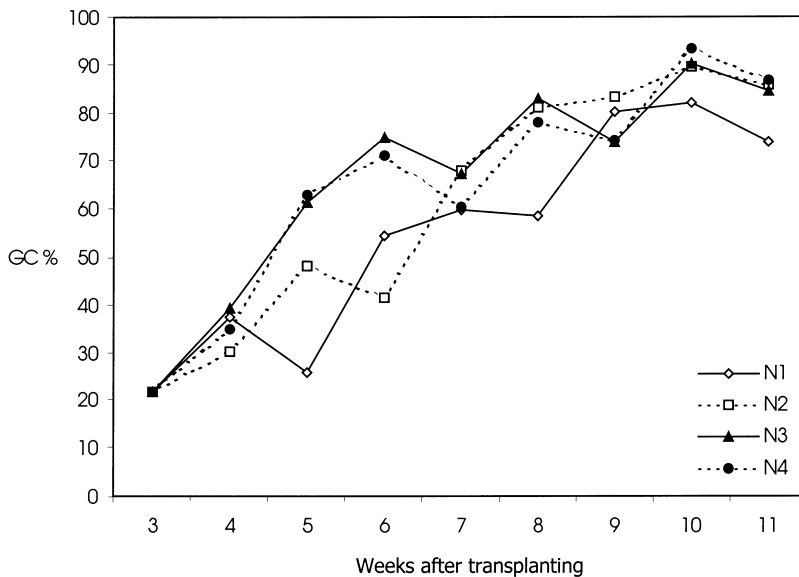


Fig. 2. Temporal profile of ground cover (GC%) during one growing season (N1–N4 are nitrogen treatments).

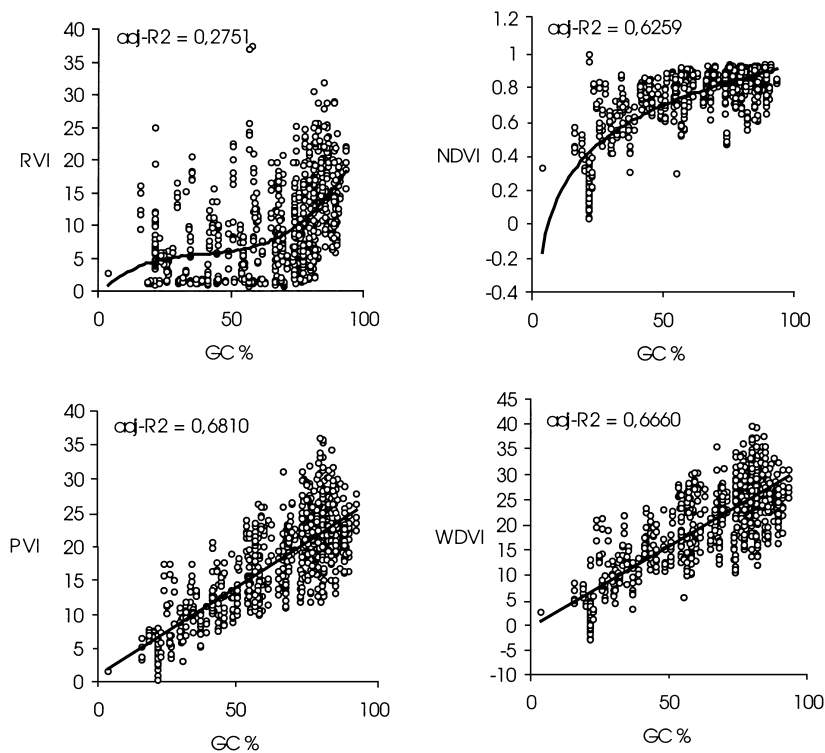


Fig. 3. Regression plots between ground cover (GC%) and RVI, NDVI, PVI, WDWI.

of Casanova were used, i.e. third-order polynomial and logarithmic models for RVI and NDVI, respectively, and simple linear models for PVI and WDWI. Fig. 3 summarizes the regression plots with their R^2 's. The final data set for modeling consisted of the data of 16 paddy plots (trial 1) with clear and disturbed water conditions, as no statistically significant difference ($P < 0.5$) was found between turbidity treatments nor between the two cultivars.

For the PVI computations, $\rho_{r,s}$ and $\rho_{ir,s}$ were assigned the values of the non-cropped plots (trial 2) averaged over the growing season. The ratio $\rho_{r,s}/\rho_{ir,s}$ in the WDWI equation was computed as the slope of the “water line” (in this case 0.62) elaborated in the second trial from the non-cropped clear and disturbed paddy plots.

The lower correlation coefficients found compared to those of Casanova may be related to the fact that Casanova did not define ground cover by digital processing of vertical downward photography, but by Fpar ceptometer measurements. The former methodology, has a serious drawback, while the choice of

training image segments for classification is photo-specific, which may have added unwanted variability to the data. Finally, only one single photo was collected per paddy plot, meaning that sampling density was limited to 1% of the plot area (m^2 out of $100 m^2$).

As the quality of ground cover data could not be warranted, in further modeling only LAI, measured at a much higher level of precision, was used as independent variable.

3.2. VIs and LAI

The course of LAI over the growing season, measured in trial 1, was smoother and more consistent than the one of ground cover (Fig. 4): LAI continuously increased with time, with a saturation towards maturity. Moreover, the effect of various N fertilization levels was clearly distinguishable.

A logarithmic transformation of LAI allowed for a linear regression analysis between the various VIs variables and LAI. The adjusted R^2 values and the regression plots presented in Fig. 5, show that the

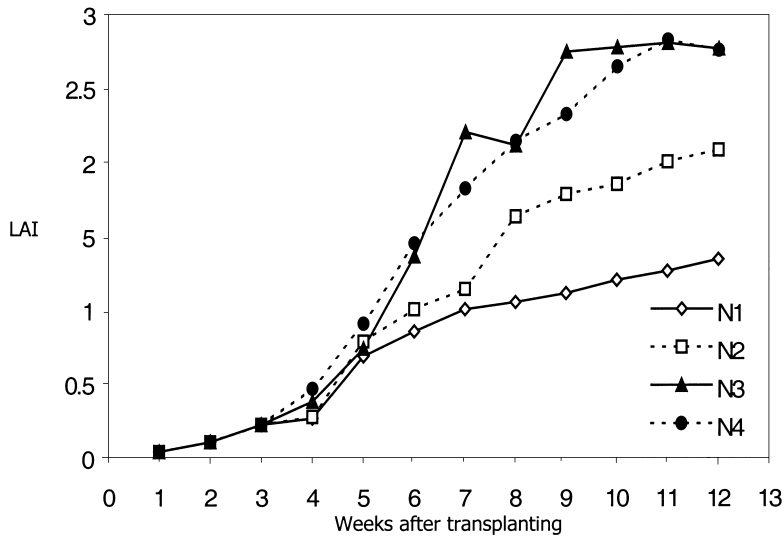


Fig. 4. Temporal profile of LAI during one growing season (N1–N4 are nitrogen treatments).

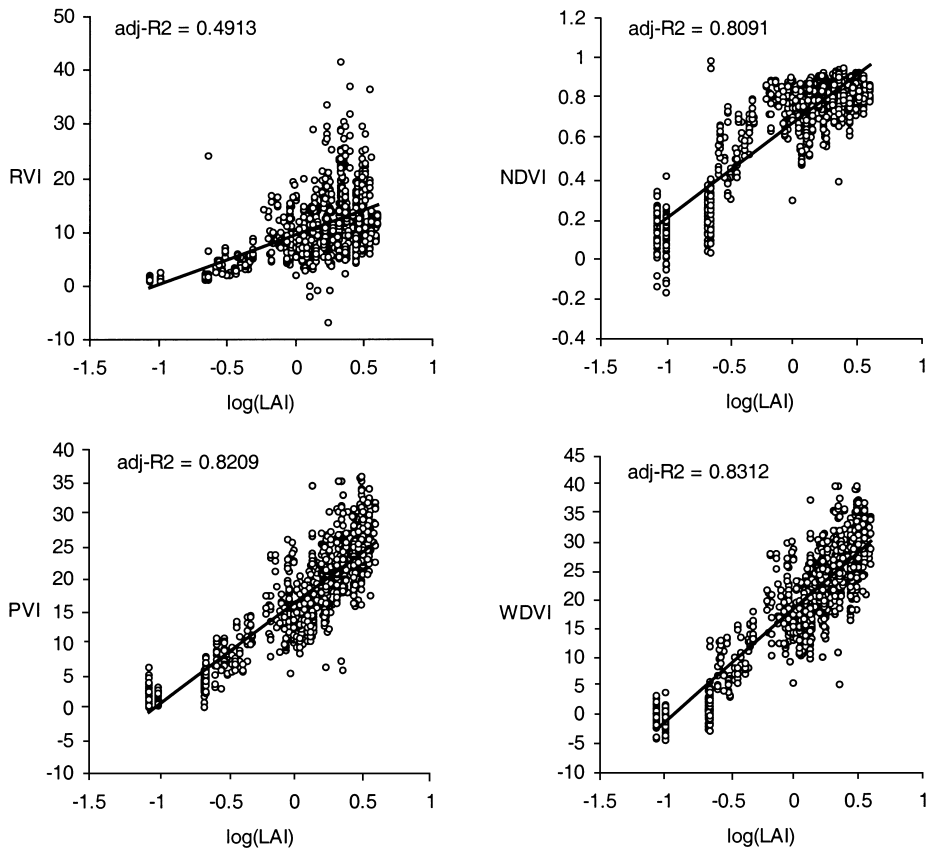


Fig. 5. Regression plots between LAI and RVI, NDVI, PVI, WDV.

Table 1
P-values for the categorical variables “turbidity”, “background color”, “cultivar” and “N treatment” in a GLM multiple regression procedure with the various VIs as independent and $\log(\text{LAI})$ as dependent variable

	<i>P</i> -value			
	Turbidity	Background color	Cultivar	N treatment
RVI	0.0697	0.0563	0.1074	0.3188
NDVI	0.0631	0.0425	0.3469	0.7713
PVI	0.8551	0.9461	0.0617	0.0936
WDVI	0.0483	0.9534	0.2167	0.1567

NDVI-, PVI- and WDVI-based models explained about twice as much variability as the RVI-based model. However, no significant difference in predictive power could be demonstrated between the former three indices.

To study the influence of rice cultivar, water turbidity, paddy depth, background color and N treatment, generalized linear model (GLM) multiple regression procedures (SAS, 1989) were applied. Table 1 summarizes the resulting *P*-values. Neither one of the four independent variables contributed significantly to the model's goodness of fit, though two variable combinations were significant at the

$\alpha = 0.05$ level: turbidity for the LAI–WDVI linear relationship and paddy background color for the LAI–NDVI linear model. Moreover, a parallel analysis on the data of trial 3 confirmed that the spectral response of paddy water was independent of its background color. We consequently pooled all data of trial 1 irrespective of rice cultivar, paddy background color, N treatment and water turbidity.

3.3. The $\log(\text{LAI})$ –VI model and other predictor variables

Other independent variables tested were water depth and average leaf chlorophyll content (ordinal data). Though the VIs used here, inherently encompass data from the red and VNIR bands, ratios may obscure information that is specific to either of these spectral channels alone. Therefore, the variables “red reflectance” and “VNIR” were as well used as independent variables.

Table 2 shows the results of the forward stepwise regression. The VNIR, the VI, the leaf chlorophyll content, red reflectance and paddy depth were ranked analogously, except in the WDVI-based model, where the red reflectance was not included. Remarkably, in two cases out of three VNIR was ranked before the VI. Probably, the positive correlation between LAI and

Table 2
 Stepwise regression results between $\log(\text{LAI})$ and explanatory variables red, VNIR, chlorophyll content, paddy depth

Step	Variable entered and removed	Number in	Partial R^{*2}	Model R^{*2}	$C(p)$	F	Probability $> F$
(a) NDVI							
1	VNIR	1	0.828	0.828	924.18	5529.61	0.0001
2	NDVI	2	0.045	0.873	379.28	411.54	0.0001
3	RED	3	0.021	0.895	126.59	230.01	0.0001
4	CHLORO	4	0.009	0.904	12.78	115.02	0.0001
5	PADDYD	5	0.000	0.905	6.00	8.78	0.0031
(b) PVI							
1	VNIR	1	0.828	0.828	238.47	5529.61	0.0001
2	CHLORO	2	0.010	0.838	156.29	74.22	0.0001
3	RED	3	0.015	0.854	36.51	118.41	0.0001
4	PVI	4	0.002	0.856	19.80	18.46	0.0001
5	PADDYD	5	0.002	0.858	6.00	15.80	0.0001
(c) WDVI							
1	WDVI	1	0.836	0.836	157.82	5851.72	0.0001
2	CHLORO	2	0.015	0.851	36.55	119.76	0.0001
3	VNIR	3	0.002	0.854	21.31	16.98	0.0001
4	PADDYD	4	0.002	0.856	5.00	18.31	0.0001

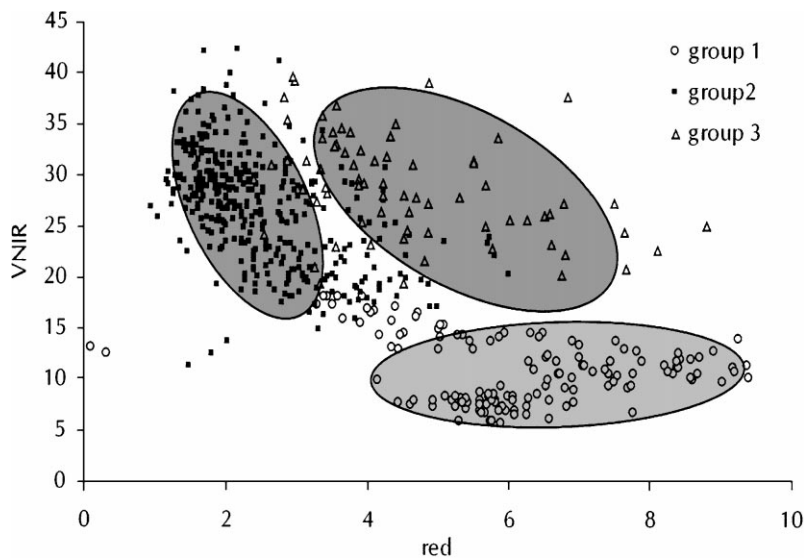


Fig. 6. Temporal variability of all spectral data.

VNIR, was accentuated because the low LAI values in the beginning of the growth cycle (corresponding to VNIR values) were reduced even more by the extreme VNIR absorption of the open water surface. The presence of algae on the water surface, on the other hand, could explain the inconsistent behavior with respect to red reflectance, which may have led to a weakening of the correlation where ratios were involved. Moreover, the explicative power of flood-water depth was demonstrated to be weak, and therefore this variable was omitted from further analysis. Leaf chlorophyll content as well explained only a small surplus in variance (R^2 increase of 0.01–0.025). It was omitted from further analysis (see Section 4) because (1) the present research was a preliminary phase to the development of models derived from spectral measures made from space-based sensors; (2) its small predictive power does not justify the enormous costs of its assessment.

3.4. Creation and inclusion of a growth-stage-dependent model variable

Fig. 6 illustrates the separation of the pooled data of trial 1 into three clusters, differentiated according to rice crop development: vegetative, reproductive and maturation stages (see also Section 3.1). The spectral behavior of group 1 resembles that of a floodwater

layer, which can be explained by the open canopy structure. Three weeks after transplanting, spectral observations had moved into group 2. Here, very-near-infrared absorption by the water layer was decreased rapidly and VNIR values increased with increasing crop cover. Moreover, total chlorophyll content strongly increased, causing a reduction in red reflectance. Group 3 corresponds to mature and senescent rice crops with decreasing chlorophyll content (shift to higher red reflectance). The wider variability in group 3 was due to different N treatments resulting in different moments of senescence and thus of chlorophyll content.

Statistical canonical discriminant analysis performed in SAS (SAS, 1989) confirmed the visual cluster differentiation both for the pooled data as for the data per N treatment. In both cases group numbers (1–3) were introduced as a classification variable. To enhance the accuracy of the discriminant analysis process, data were added on the blue (centered at $0.46 \mu\text{m}$) and green (centered at $0.56 \mu\text{m}$) reflectance to the quantitative dataset.

The multivariate statistic probabilities in Table 3 demonstrate that the group mean values are identical in a four-dimensional space. The three groups can therefore statistically be distinguished using the group number as classification variable. The canonical structure confirms that the VNIR reflectance (highest

Table 3

Summary of the CANDISC procedure for the pooled data (group number: classification variable; blue, green, red, VNIR: quantitative variables)

Statistic	F-value	Num DF	Den DF	Probability > F	
<i>Multivariate statistics and F-approximations (S = 2, M = 0.5, N = 569.5)</i>					
Wilks' lambda	0.18661	375.07	8	2282	0.0001
Pillai's trace	1.04228	310.70	8	2284	0.0001
Hotelling–Lawley trace	3.13212	446.32	8	2280	0.0001
Roy's greatest root	2.67329	763.22	4	1142	0.0001
Total canonical structure					
	CAN1	CAN2			
Red	0.83147	0.53283			
Green	0.43286	0.76418			
Blue	0.73551	0.31035			
VNIR	−0.94317	0.25613			
Group	Class means on canonical variables				
	CAN1	CAN2			
1	2.85176	−0.08885			
2	−0.99429	−0.32682			
3	−0.62182	1.72490			

absolute value) supports the discrimination (maximized by CAN1) best. According to the class means sub-table, the following canonical variables separated groups maximally: CAN1 for group 1 vs. groups 2 and 3, and CAN2 for group 3 vs. groups 2 and 1.

The inclusion of the growth-stage-dependent variable “group number” to the log(LAI)–VI/red/VNIR model resulted in an increase of adjusted R^2 's up to a maximum of 0.93 (Table 4).

The same procedures were applied to the data of the four N treatments separately, with the same results as for the pooled dataset. This observation corresponds to the weak explicative power of the variable “N treatment” demonstrated previously. Crop status variability due to different N treatments is explained by the different spectral indices, whereas an additional variable that directs the spectral indices in temporal space results in better predictive models.

Table 4

Multiple regression output with log(LAI) as dependent variable and as independent variables: red, VNIR, group number

Source	DF	Sum of squares	Mean square	F-value	Probability > F
(a) NDVI					
Model	5	1357.17	271.43	3056.58	0.0001
Error	1141	101.32	0.08		
Adjusted R^2	0.930				
(b) PVI					
Model	5	1336.59	267.31	2502.02	0.0001
Error	1141	121.90	0.10		
Adjusted R^2	0.916				
(c) WdVI					
Model	4	1334.93	333.73	3084.19	0.0001
Error	1142	123.57	0.10		
Adjusted R^2	0.915				

3.5. Model adaptability to space-based remote sensing

The present study demonstrates that further research on adapting models making use of spectral information to predict paddy rice crop status to satellite-based sensors is warranted. However, its usefulness depends on the spectral, temporal and spatial resolution of the satellite sensor as well as on the objectives of using these satellite sensors (e.g. for inter-seasonal vs. intra-seasonal monitoring, for water management purposes vs. yield prediction purposes, ...). Although this study proved that only spectral information furnishes information on the vegetation properties of paddy rice, i.e. LAI and growth-stage (irrespective of N treatment), extrapolation to satellite-level still will require ground measurements. For example, ground measured reflectances will be needed for satellite sensor data calibration, GPS readings for georeferencing satellite images and a certain amount of LAI-measurements for continuous cross-verification. Still, we believe that the intrinsic advantages of satellite-based crop monitoring (i.e. monitoring crops on a regional scale, resulting in a high cost-effectiveness) will compensate for the latter drawbacks.

4. Conclusion

Our results demonstrated that spectral information can provide acceptable estimates of LAI where it concerns paddy rice cultures. This does not hold for ground cover, which was probably due to inaccuracy in ground cover field data collection.

The presence of a floodwater layer affected relationships between LAI and spectral + biophysical parameters only in one way: probably due to the occurrence of algae on the water surface of the flooded paddies (which is also often the case in real world situations), the single VNIR band explained more model variability than NDVI, PVI and WDVI.

The relationships were not affected by rice cultivar, paddy background color, N treatment, water turbidity level and floodwater depth. Average leaf chlorophyll content contributed significantly, although not strongly, to model predictive power. The inclusion of a categorical growth-stage-dependent variable, derived from the temporal variability of red/VNIR

spectral signatures of the paddy rice, improved the models significantly. The predictive power of this variable was not affected when it was derived for each N treatment separately.

Though reflectances were grouped arbitrary (based upon the visually discernable stages of rice crop development), it is possible to implement this in a more rigorous manner based on the phenological stages of rice as described by Yoshida (1981).

However, models developed in the present study can serve as a basis for developing satellite-based paddy rice monitoring systems.

References

- Bouman, B.A.M., 1995. Crop modeling and remote sensing for yield prediction. *Neth. J. Agric. Sci.* 43, 143–161.
- Bouman, B.A.M., Kasteren, H.W.J., van Uenk, D., 1992. Standard relations to estimate ground cover and LAI of agricultural crops from reflectance measurements. *Eur. J. Agric.* 1, 249–262.
- Casanova, D., Epema, G.F., Goudriaan, J., 1998. Monitoring rice reflectance at field level for estimating biomass and LAI. *Field Crops Res.* 55, 83–92.
- Clevers, J.G.P.W., 1989. The application of a weighted infrared-red vegetation index for estimating leaf area index by correcting for soil moisture. *Remote Sensing Environ.* 29, 25–37.
- Clevers, J.P.G.W., Verhoef, W., Buiten, H.J., Leeuwen, H.J.C., Maren, C., Varenkamp, C., Rijckenberg, G.J., 1991. Modeling and synergetic use of optical and microwave remote sensing. Report 2. LAI estimate from canopy reflectance and WDVI: a sensitivity analysis with the SAIL model. BCRS.
- Cropscan Inc, 1993. Multispectral Radiometer (MSR): User's Manual and Technical Reference. CropScan Inc, Rochester.
- FAOSTAT, 1998. <http://apps.fao.org>.
- Gallo, K.P., Daughtry, C.S.T., Bauer, M.E., 1985. Spectral estimate of absorbed photosynthetically active radiation in corn canopies. *Remote Sensing Environ.* 17, 221–232.
- Gilbert, M.A., Meliá, J., 1990a. Usefulness of the temporal analysis and the normalized difference in the study of rice by means of Landsat-5 TM images: identification and inventory of rice fields. *Geocarto Int.* 5, 17–26.
- Gilbert, M.A., Meliá, J., 1990b. Usefulness of the temporal analysis and the normalized difference in the study of rice by means of Landsat-5 TM images: establishment of relationships for yield prediction purpose. *Geocarto Int.* 5, 27–32.
- Huete, A.R., Jackson, R.D., 1985. Spectral response of a plant canopy with different soil backgrounds. *Remote Sensing Environ.* 17, 37–53.
- Idrisi, Eastman, R.J., 1997. *Idrisi for Windows User's Guide* by Eastman. Clark University, Worcester, MA.
- Ishiguro, E., Kumar, M.K., Hidaka, Y., Yoshida, S., Sato, M., Miyazato, M., Chen, J.Y., 1993. Use of rice response characteristics in area estimate by LANDSAT/TM and MOS-1 satellites data. *ISPRS J. Photogram.* 48, 26–32.

- Kumar, M., Montheith, J.L., 1981. Remote Sensing of Crop Growth. *Plants and Daylight Spectrum*. Academic Press, London, pp. 133–144.
- Leblon, B., Guerif, M., Baret, F., 1991. The use of remotely sensed data in estimate of PAR use efficiency and biomass production of flooded rice. *Remote Sensing Environ.* 38, 147–158.
- Licor, 1990. LAI-3000 Plant Canopy Analyzer Instruction Manual. Lincoln, Licor Inc., Nebraska.
- Licor, 1992. LAI-2000 Plant Canopy Analyzer Instruction Manual. Lincoln, Licor Inc., Nebraska.
- Neter, J., Kutner, M.H., Nachtsheim, C.J., Wasserman, W., 1996. *Applied Linear Statistical Models*. Irwin, IL.
- Patel, N.K., Singh, T.P., Sahai, B., Patel, M.S., 1985. Spectral response of rice crop and its relation to yield and yield attributes. *Int. J. Remote Sensing* 6, 657–664.
- Rouse, J.W. Jr., Haas, R.H., Schell, J.A., Deering, D.W., 1973. Monitoring vegetation systems in the Great Plains with ERTS. In: *Proceedings of the Earth Research Technical Satellite-1 Symposium*. Goddard Space Flight Center, Washington, DC, pp. 309–317.
- Salvador, R., Pons, X., 1998. On the reliability of Landsat TM for estimating forest variables by regression: a methodological analysis. *IEEE Trans. Geosci. Remote Sensing* 36, 1888–1897.
- SAS, 1989. *SAS/STAT User's Guide*, Vol. 1, 4th Edition.
- Steven, M.D., Biscoe, P.V., Jaggard, K.W., 1985. Estimate of sugar beet productivity from reflection in the red and infrared spectral bands. *Int. J. Remote Sensing* 4, 325–334.
- ten Berge, H.F.M., Riethoven, J.J.M., Wopereis, M.C.S., 1995. Numerical optimization of nitrogen fertilizer use in irrigated rice. DLO-Research Institute of Agrobiolgy and Soil Fertility, Wageningen, and International Rice Research Institute, Los Baños.
- Wallace, J.F., Campbell, H., 1989. Analysis of Remotely Sensed Data. *Remote Sensing of Biosphere Functioning*. Springer, New York, pp. 297–304.
- Wiegand, C.L., Richardson, A.J., 1987. Spectral components analysis: rationale and results for three crops. *Int. J. Remote Sensing* 8 (7), 1011–1032.
- Yoshida, S., 1981. *Fundamentals of rice crop science*. International Rice Research Institute, Los Baños.